Neurobiology of Aging 105 (2021) 241–251

Contents lists available at ScienceDirect

Neurobiology of Aging

journal homepage: www.elsevier.com/locate/neuaging.org

Regional relationships between CSF VEGF levels and Alzheimer's disease brain biomarkers and cognition

Meral A. Tubi[a], Deydeep Kothapalli[a], Matthew Hapenney[a], Franklin W. Feingold[a,b], Wendy J. Mack[c], Kevin S. King[d], Paul M. Thompson[a], Meredith N. Braskie[a,*], for Alzheimer's Disease Neuroimaging Initiative[**]

[a] *Imaging Genetics Center, Mark and Mary Stevens Neuroimaging and Informatics Institute, Keck School of Medicine, University of Southern California, Marina del Rey, CA, USA*
[b] *Stanford University, Stanford, CA 94305*
[c] *Division of Biostatistics, Department of Preventive Medicine, University of Southern California, Los Angeles, CA, USA*
[d] *Huntington Medical Research Institutes, Imaging Division, Pasadena, CA, 91105 USA*

ARTICLE INFO

Article history:
Received 22 January 2021
Revised 22 April 2021
Accepted 24 April 2021
Available online 21 May 2021

Keywords:
FDG-PET
MRI
Cortical thickness
Executive function
Amyloid-beta
Tau
Vascular endothelial growth factor

ABSTRACT

Vascular endothelial growth factor (VEGF) is a complex signaling protein that supports vascular and neuronal function. Alzheimer's disease (AD) -neuropathological hallmarks interfere with VEGF signaling and modify previously detected positive associations between cerebral spinal fluid (CSF) VEGF and cognition and hippocampal volume. However, it remains unknown 1) whether regional relationships between VEGF and glucose metabolism and cortical thinning exist, and 2) whether AD-neuropathological hallmarks (CSF Aβ, t-tau, p-tau) also modify these relationships. We addressed this in 310 Alzheimer's Disease Neuroimaging Initiative (ADNI) participants (92 cognitively normal, 149 mild cognitive impairment, 69 AD; 215 CSF Aβ+, 95 CSF Aβ-) with regional cortical thickness and cognition measurements and 158 participants with FDG-PET. In Aβ + participants (CSF $A\beta_{42} \leq 192$ pg/mL), higher CSF VEGF levels were associated with greater FDG-PET signal in the inferior parietal, and middle and inferior temporal cortices. Abnormal CSF amyloid and tau levels strengthened the positive association between VEGF and regional FDG-PET indices. VEGF also had both direct associations with semantic memory, as well as indirect associations mediated by regional FDG-PET signal to cognition.

1. Introduction

Vascular endothelial growth factor-A (VEGF), a signaling protein encoded by the *VEGF-A* gene, is involved in vascular and metabolic physiological processes including blood vessel growth, oxygen and glucose delivery, vasodilation, and vascular permeability (Lange et al., 2016). Homeostatic VEGF signaling is also integral to the maintenance of cognitive function (Cao et al., 2004), as VEGF promotes neurogenesis (Cao et al., 2004; Fournier et al., 2012), improves synaptic plasticity (Licht et al., 2011), and counteracts neurodegeneration (Gora-Kupilas and Josko, 2005; Zacchigna et al., 2008) - all essential to the preservation of cognitive ability in older adults.

Greater VEGF availability is neuroprotective in pre-clinical Alzheimer's disease (AD) models (Religa et al., 2013; Spuch et al., 2010; Wang et al., 2011), but *in-vivo* human studies have found varying relationships between VEGF levels and AD diagnosis and cognition. Specifically, in small independent studies, cerebrospinal fluid (CSF) VEGF levels did not differ by diagnosis (Chakraborty et al., 2018) or were higher in AD patients compared to controls (Tarkowski et al., 2002). However, in larger Alzheimer's Disease Neuroimaging Iniative (ADNI) studies, higher CSF VEGF levels were associated with less cognitive decline (Hohman et al.,

Conflicts of interest: The authors do not have financial interests or conflicts of interest related to the topic of the paper.

* Corresponding author at : Imaging Genetics Center, Mark and Mary Stevens Neuroimaging and Informatics Institute, Keck School of Medicine, University of Southern California, 4676 Admirality Way Marina Del Rey, 90292, Tel: (323) 442-7246; fax: (323) 442-7247.

E-mail addresses: braskie@usc.edu, tubi@usc.edu (M.N. Braskie).

** Data used in preparation of this article were obtained from the Alzheimer's Disease Neuroimaging Initiative (ADNI) database (adni.loni.usc.edu). As such, the investigators within the ADNI contributed to the design and implementation of ADNI and/or provided data but did not participate in analysis or writing of this report. A complete listing of ADNI investigators can be found at: http://adni.loni.usc.edu/wpcontent/uploads/how_to_apply/ADNI_Acknowledgement_List.pdf

0197-4580/$ – see front matter © 2021 Elsevier Inc. All rights reserved.
https://doi.org/10.1016/j.neurobiolaging.2021.04.025

2015; Paterson et al., 2014) and this relationship was stronger in those with abnormal levels of AD-neuropathological hallmarks - CSF $A\beta_{42}$ and CSF t-tau (Hohman et al., 2015).

The association between VEGF and cognition may be stronger in the presence of AD pathology, possibly due to bidirectional effects between VEGF and amyloid and tau on brain function. Amyloid can modify homeostatic VEGF signaling; for instance, in AD human post-mortem temporal cortex tissue samples, VEGF co-accumulated with pre-aggregated $A\beta$ plaques with a high affinity and specificity to $A\beta$ peptides, ultimately depleting VEGF bioavailability (Yang et al., 2004). $A\beta$ can also interfere with VEGF signaling by modifying VEGF receptor expression (Angom et al., 2019; Cho et al., 2017). Conversely, higher VEGF levels, generated through exogenous application of VEGF, can also rescue vascular damage, attenuate memory impairment when it exists, and reduce amyloid and hyperphosphorylated tau load (Religa et al., 2013). Thus, presence of higher VEGF levels may compensate for amyloid-driven VEGF inhibition, resulting in better brain function and cognitive ability. While the relationship between VEGF and tau has not been fully elucidated, a recent animal tauopathy model demonstrated that tau induced blood vessel abnormalities with an associated up-regulation of *VEGF-A* gene expression (Bennett et al., 2018). Collectively, these studies highlight both independent and synergistic relationships between VEGF and AD neuropathological hallmarks, but it remains unknown whether these interactions exist for early brain biomarkers on the AD cascade, such as cerebral glucose metabolism and cortical thickness.

By the time an individual has evidence of cognitive decline and/or an AD diagnosis, the brain has already undergone severe structural and functional degeneration, making it essential to assess factors, such as VEGF, that may contribute to brain biomarker changes early in the AD cascade. Neuroimaging brain biomarkers fluctuate early and follow a specific spatial and temporal sequence in disease course (Jack and Holtzman, 2013). Identifying the spatial relationship of vascular factors to brain measures may also illuminate possible vascular mechanisms that contribute to heterogeneity in AD neuroimaging phenotype patterns (Risacher et al., 2017). Critically, few studies have mapped how human VEGF levels are related to early AD-brain biomarkers. Data derived from the ADNI indicate that higher CSF VEGF levels are associated with less hippocampal atrophy and greater total cerebral glucose metabolism (Hohman et al., 2015; Wang et al., 2018), but regional cortical indices of glucose metabolism and gray matter thickness have yet to be identified. Mapping these regional relationships will help clarify how VEGF relates to the topographical trajectory of AD-related pathology and disease progression, informing future mechanistic and prevention studies.

To address these gaps, we evaluated whether CSF VEGF levels were related to regional measures of 1) flurodeoxyglucose (FDG) positron emission tomography (PET) and 2) and magnetic resonance imaging (MRI) derived cortical thickness in AD-signature regions (Wang et al., 2015), by assessing these associations in both $A\beta+$ and $A\beta-$ participant subgroups (Shaw et al., 2009) in an ADNI cohort (N = 310). We also evaluated whether these regional associations were modified by CSF $phosphorylated_{181}$ tau (p-tau), an AD-specific marker of tau phosphorylation, and total tau (t-tau), a non-specific marker of neuronal damage that is closely linked to cognitive dysfunction in early stages of AD (Blennow et al., 2010; Hedden et al., 2013; Holtzman, 2011). We hypothesized that in those along the AD-continuum (i.e., $A\beta+$ participants), higher endogenous VEGF levels (which may compensate for amyloid-driven VEGF inhibition) would be associated with greater glucose metabolism and cortical thickness in AD-signature regions. Whereas in $A\beta-$ participants, we hypothesized that higher endogenous VEGF levels would not be positively associated with AD-brain biomarkers, since a lower amyloid load would likely not interfere with VEGF availability. Since abnormal tau accumulation is more closely linked to changes in brain function and cognitive decline in AD than amyloid (Hedden et al., 2013; Ossenkoppele et al., 2019), we hypothesized that the association between VEGF levels and AD-relevant brain neuroimaging biomarkers would be strongest in the presence of higher CSF p-tau and t-tau levels.

In a secondary analysis, we reproduced a previous analysis by Hohman et al., (Hohman et al., 2015) that evaluated the relationships between VEGF levels and cognitive domain measures of executive function (ADNI-EF) and episodic memory (ADNI-MEM). We further expanded on the analysis by assessing test-specific effects in cognitive domain measures. We also evaluated whether the previously-detected association between VEGF and cognition was mediated by regional FDG-PET associations. We hypothesized that regional FDG-PET signal would mediate the detected association between VEGF and cognition in those along the AD continuum ($A\beta+$ participants).

2. Methods

2.1. The Alzheimer's Disease Neuroimaging Initiative (ADNI)

Data used in the preparation of this article were obtained from the Alzheimer's Disease Neuroimaging Initiative (ADNI) database (adni.loni.usc.edu). The ADNI was launched in 2004 as a public-private partnership, led by Principal Investigator Michael W. Weiner, MD. The primary goal of ADNI has been to test whether serial magnetic resonance imaging (MRI), PET, other biological markers, and clinical and neuropsychological assessment can be combined to measure the progression of mild cognitive impairment (MCI) and early AD. For up-to-date information, see www.adni-info.org. All data utilized in this study were acquired from the publicly available ADNI Image Data Archive (https://ida.loni.usc.edu).

2.2. Participants

We selected participants from the ADNI cohort who had available CSF VEGF, 1.5 T structural MRI scan, and neuropsychological assessment within 1 year of each other, resulting in 310 participants (92 cognitively intact (CI), 149 mild cognitive impairment (MCI), 69 AD), aged 56 to 89 years old. CSF was acquired within a mean ± standard deviation (SD) of 28.6 ± 28.5 days (max = 237 days) from the MRI scan. Neuropsychological assessments were acquired within a mean ± SD of 18.6 ± 24.5 days (max = 237 days) from the MRI scan. In a subset of the cohort, we analyzed 158 participants who also underwent FDG-PET scanning (39 CI, 80 MCI, 39 AD) acquired within a mean ± SD of 30.0 ± 26.7 (max = 203 days) days from the MRI scan.

Detailed information on ADNI's participant selection and diagnostic criteria are outlined in the ADNI protocol (http://www.adni-info.org/Scientists/AboutADNI.aspx). Briefly, participants were excluded from the ADNI cohort if they had a serious neurological or neuropsychiatric condition, or history of brain injury. Participants were classified into diagnostic categories of probable AD, MCI, and CI. Criteria for an AD diagnosis included: 1) a memory complaint, 2) objective memory dysfunction identified by an education-adjusted Wechsler Memory Scale-Revised (WMS-R) - Logical Memory II (LM-II) R (WMS-R LM-II), 3) Mini-Mental State Exam (MMSE) score between 20-26 (inclusive), 4) Clinical Dementia Rating (CDR) $\geq$ 0.5), and 5) NINDS/ADRDA criteria for probable AD (McKhann et al. 1984). MCI diagnosis was made when 1) a reported memory complaint was present, but the diagnostic criteria for dementia was not met, or 2) when they scored between 24-30

Table 1
Participant Characteristics

	Total Cohort	Aβ+	Aβ-	p-value
N	310	215	95	
Age (years)	74.8 ± 6.8	74.6 ± 6.9	75.5 ± 6.6	0.60
Sex				0.65
Males	187 (60.3%)	132 (61.4%)	55 (57.9%)	
Females	123 (39.7%)	83 (38.6%)	40 (42.1%)	
Diagnosis				< 0.001*^
Cognitively intact (CI)	92 (29.7%)	33 (15.3%)	59 (62.1%)	
Mild cognitive impairment (MCI)	149 (48.1%)	117 (54.4%)	32 (33.7%)	
Alzheimer's disease (AD)	69 (22.2%)	65 (30.2%)	4 (4.2%)	
Apolipoprotein ε4 (*APOE*4) allele count			< 0.001*^	
0 *APOE*4 alleles	159 (51.3%)	74 (34.4%)	85 (89.5%)	
1 *APOE*4 alleles	115 (37.1%)	105 (48.8%)	10 (10.5%)	
2 *APOE*4 alleles	36 (11.6%)	36 (16.7%)	0 (0.0%)	
Education (years completed)	15.7 ± 3.0	15.6 ± 3.0	15.8 ± 2.8	0.88
MMSE score	26.8 ± 2.6	26.1 ± 2.6	28.4 ± 1.7	< 0.001*^
CSF VEGF (natural log of pg/mL)	2.70 ± 0.13	2.69 ± 0.13	2.74 ± 0.13	< 0.001*^
CSF t-tau (pg/mL)	98.4 ± 52.1	113.8 ± 54.4	63.4 ± 20.5	< 0.001*^
CSF p-tau (pg/mL)	33.9 ± 17.4	39.7 ± 17.3	20.9 ± 7.6	< 0.001*^

Continuous variables shown as mean ± standard deviation. Categorical variables shown as frequency (%). Amyloid group level differences (Aβ- vs. Aβ+) were evaluated on continuous variables using a Welch's two-sample t-test and categorical variables using a χ^2 test. * indicates $p < 0.05$ group difference between Aβ- (n=95) vs. Aβ+ (n=215) participants. ^ indicates $p < 0.05$ between Aβ- (n=42) vs. Aβ+ (n=116) participants in subset with available FDG-PET data.

(inclusive) on the MMSE and 0.5 on the CDR (with CDR memory box score 0.5 or higher). CI participants did not meet the criteria for probable AD or MCI and had no memory complaints. Participant characteristics are detailed in Table 1.

2.3. CSF analytes

All CSF analyte measurements were previously analyzed by others and accessed through ADNI's publicly available data repository (htttp://adni.loni.usc.edu). In this analysis, CSF analytes used were VEGF-A, amyloid-beta$_{42}$ (Aβ), total-tau (t-tau), and phosphorylated$_{181}$-tau (p-tau). CSF samples were acquired at the baseline visit and were batch processed using Luminex Multi-Analyte Profiling (xMAP) immunoassay technology (Myriad Rules Based Medicine; RBM, Austin, TX), with standard ADNI protocols (Spellman et al., 2015). We used the ADNI CSF Aβ and total t-tau quality-checked median scaled analyte measurements. Clinical performance of these analytes was previously assessed in a precision analysis conducted in an inter-laboratory standardization study across seven centers using five CSF pools from 3 cognitively normal older adults and 2 AD patients (Shaw et al., 2011). All samples were run in duplicate. Amyloid positivity was defined by cut-offs outlined in prior work; Aβ+ individuals had CSF Aβ$_{42}$ <192 pg/mL and Aβ- participants had CSF Aβ$_{42}$ levels ≥192 pg/mL (Shaw et al., 2009). Quality control (QC) procedures for CSF Aβ$_{42}$, CSF p-tau, and t-tau are described elsewhere (Shaw et al. 2009; Shaw et al. 2011).

We downloaded CSF VEGF values from ADNI Biomarkers Consortium CSF QC Multiplex data sheet. The CSF samples were acquired from participants after an overnight fast at the ADNI 1 baseline visit. The samples were processed, aliquoted, and stored at -80°C in accordance with ADNI Biomarker Core Laboratory Standard Operating Procedures (http://adni.loni.usc.edu/wp-content/uploads/2010/09/CSF_Biomarker_Test_Instr.pdf). The QC procedures performed by ADNI on the CSF VEGF assay (and all ADNI CSF proteomic assays) included test/retest on a subsample of 16 CSF samples to test for the precision, cross-reactivity, spike-recovery (accuracy), and reliability. No missing data and no outliers were reported for CSF VEGF values, according to ADNI Biomarkers Consortium CSF QC multiplex data. VEGF measurements were natural log-transformed by ADNI (Box and Cox, 1964).

2.4. APOE genotyping

We adjusted for Apolipoprotein E ε4 (*APOE*4) genotype in all analyses. *APOE*4 genotype count was coded as 0 for *APOE*4 non-carriers, 1 for carriers of one *APOE4* allele, and 2 for carriers of two *APOE*4 alleles. We coded by dose because of possible dose-dependent effects of *APOE*4 on cognitive ability, vascular function, and MRI biomarkers (Makkar et al. 2020; Hobel et al. 2018). *APOE* genotyping was performed by Cogenics from a 3mL aliquot of blood. PCR amplification and Hhal restriction enzyme digestion was performed, which was then resolved on 4% Metaphor Gel and viewed by ethidium bromide staining (Saykin et al., 2010). More information on the ADNI *APOE* genotyping protocol can be found here: http://adni.loni.usc.edu/methods.

2.5. MRI processing

All participants underwent MRI scanning of a sagittal T1-weighted 3D Magnetization Prepared Rapid Acquisition Gradient Echo (MPRAGE) at 1.5 T, acquired across 55 sites. Scans were conducted and coordinated across sites for optimal comparability according to ADNI protocols (http://adni.loni.usc.edu/methods/documents/mri-protocols/) and passed quality control (QC) (Wyman et al. 2012). We processed MRIs with FreeSurfer 5.3 (http://surfer.nmr.mgh.harvard.edu/) (Dale et al., 1999; Fischl and Dale, 2000) to calculate regional cortical thickness in *a-priori* selected regions-of-interest (ROI) in an AD-cortical thinning signature: the entorhinal cortex (ERC), posterior cingulate, superior (STG), middle (MTG), and inferior temporal gyri (ITG), fusiform gyri, superior and inferior parietal cortex, and precuneus (Wang et al., 2015). AD signature ROIs are visualized in Figure 1. These ROIs were selected as they detect subtle and early neuronal loss, correlate spatially with tau progression and cognitive decline (Burggren et al., 2008; Querbes et al., 2009; Wang et al., 2015). All individual regions were visually quality checked and regional cortical thickness measures that failed our QC protocol were excluded from the study. Raters (n = 2) performed a test for QC on a known

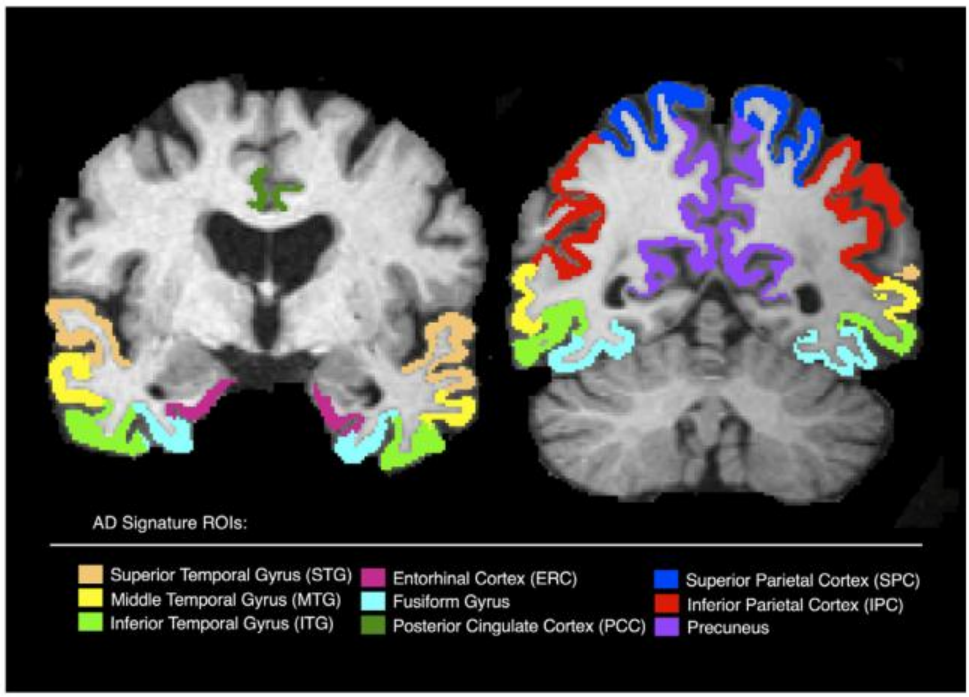

Fig. 1. AD-signature ROIs extracted from FreeSurfer mapped on a skull-stripped brain.

training set and were required to obtain reliability indicating substantial agreement (Cohen's $\kappa > 0.60$) to the answer key before performing quality checks in the current study.

2.6. FDG-PET processing

158 participants (39 CI, 80 MCI, 39 AD) underwent a fasting FDG-PET scan at their baseline visit, using a standard protocol (six 5-minute frames collected 30 minutes after a 5 mCi [^{18}F]-FDG injection) (Jagust et al., 2010). We downloaded pre-processed FDG-PET scans (Co-registered, Averaged, Standardized Image and Voxel Size, Uniform Resolution), from the LONI IDA website (https://ida.loni.usc.edu). FDG-PET pre-processing was performed according to standardized protocols to reduce inter-scanner effects (Joshi et al., 2009) and enable data pooling. Pre-processing steps included averaging the frames and spatially aligning (via interpolation) to a standard voxel size and resolution.

We constructed a study-specific minimum deformation template (MDT) to reduce the total deformation effort needed to co-register images. The MDT was constructed from T1-weighted 3D MPRAGE scans derived from 26 non-demented (11 CI, 15 MCI) participants from our sample. MDT construction has been previously described (Braskie et al., 2014). Briefly, we linearly transformed the skull-stripped T1-weighted MPRAGE scans into a standard template space. Next, an affine template was created by taking the voxelwise average of the aligned scans. The scans were then iteratively, nonlinearly transformed to the affine template (Yanovsky et al., 2009; Yanovsky et al., 2008).

FDG-PET voxelwise intensity values were divided by a pons-vermis mean reference region value - defined as the top 50% of the pons and cerebellar vermis on corresponding slices, as recommended for cross-sectional FDG-PET analyses (Landau et al., 2012). We manually segmented the reference region in MNI standard template space, guided by an atlas (Cerebellum MNIfnirt-maxprob-thr50-1mm) and subsequently performed linear and nonlinear transformations using FMRIB's Linear Image Registration Tool (FLIRT) in FSL (Jenkinson and Smith, 2001; Jenkinson et al., 2002) and ANTs symmetric image normalization (SyN) method (Avants et al., 2008; Avants et al., 2011). ROIs were defined by the same FreeSurfer AD-signature ROIs listed in Figure 1and co-registered to the participant's FDG-PET scan through linear and nonlinear transformations. After all co-registrations passed visual QC inspection, the mean FDG-PET standard uptake value ratio (SUVR) of each AD-signature ROI was extracted.

2.7. Neuropsychological assessment

Validated neuropsychological composite measures of executive function (ADNI-EF) and memory (ADNI-MEM) were used to assess domain-specific cognitive function (Crane et al., 2012; Gibbons et al., 2012). The composite measures were developed using item-response theory (IRT) and were normalized to a mean of 0 and variance of 1. ADNI-EF was derived from Trail Making Test parts A and B, Digit Span Backwards tests from the Wechsler Adult Intelligence Scale-Revised (WAIS-R), Digit Symbol Substitution, Category Fluency - Animals, Category Fluency – Vegetables, and the Clock Drawing test. ADNI-MEM was derived from the Rey Auditory Verbal Learning Test (RAVLT), the AD Assessment Schedule-Cognition (ADAS-COG), the MMSE, and Wechsler Logical Memory I and II. While composite measures have the benefit of limiting multiple comparisons, thus boosting the power to detect effects, composite measures also have limitations. For instance, ADNI-EF may mask effects of interest, such as processing speed, that occur when a cognitive domain includes heterogeneous components (Jurado and Rosselli, 2007). Therefore, our study sought to address the limitations of domain-specific assessment and expand on the analysis between ADNI VEGF levels and neuropsychological composite measures (Hohman et al., 2015) to identify test-specific associations in each subtest included in the composite measure.

2.8. Statistical analyses

2.8.1. Relationship between VEGF and Aβ levels

We conducted all statistical analyses in RStudio version 1.0.136 (http://www.R-project.org/) (University of Auckland, Auckland,

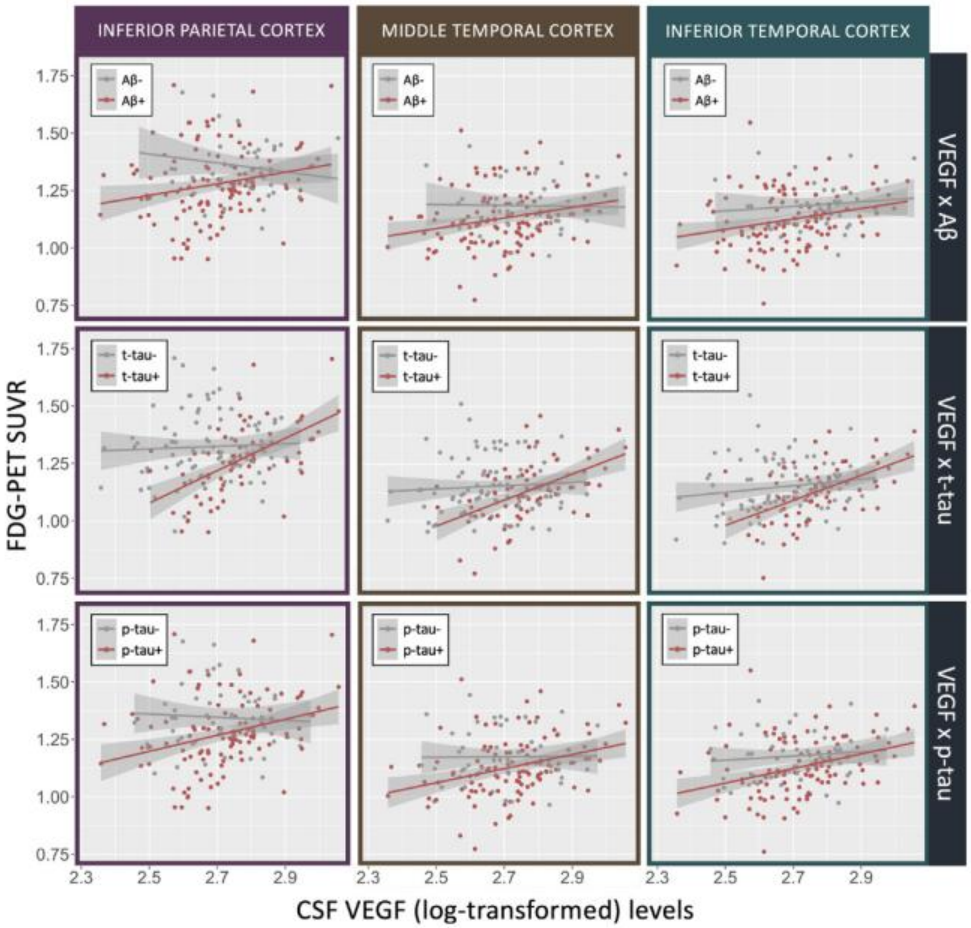

Fig. 2. Correlation plots between VEGF and FDG-PET SUVR in the inferior parietal cortex, MTG, and ITG, stratified by CSF amyloid (< 192 pg/mL), t-tau (> 93 pg/mL), and p-tau positivity (> 23 pg/mL).

New Zealand) (R Core Development Team, 2010). We stratified the cohort by CSF amyloid level (Aβ-, Aβ+) and evaluated amyloid group differences in participant characteristics using a χ^2 test for categorical variables and a Welch's two-sample t-test for continuous variables (Table 1). We also compared VEGF levels by amyloid and t-tau positivity groups (*Supplementary Figure S1*). We also evaluated whether CSF Aβ levels were significantly associated with VEGF (log-transformed) values using linear regression with spline modeling with a knot at 192 pg/ml (i.e., the threshold for amyloid positivity) (*Supplementary Figure S2*). We included age, sex, diagnosis, years of education, CSF t-tau, and *APOE*4 allele count in the model to identify associations between these variables and VEGF (log transformed) values in the entire cohort (N = 310), as well as in Aβ+ (n = 215), and Aβ- groups (n = 95) separately (*Supplementary Table S1*).

2.8.2. VEGF associations with AD brain biomarkers: FDG-PET & MRI cortical thickness ROIs

We performed all primary analyses separately in Aβ- and Aβ+ participants to separate individuals who are on the AD continuum and to identify associations relevant to AD pathogenesis. Statistical rationale also supported analyzing associations separately by Aβ-stratum because 1) CSF Aβ levels in this study have a bi-model distribution, and 2) there are far fewer Aβ- participants than there are Aβ+ participants. Moreover, since interaction tests are notoriously of low statistical power, we sought to detect more subtle differences in associations between groups by analyzing Aβ-groups separately. However, we also formally tested for statistical interactions using continuous Aβ values.

In each Aβ-stratum analysis, we used a linear mixed effects model to evaluate regional associations between VEGF (log transformed) values and each FDG-PET SUVR ROI (Table 2) and each cortical thickness ROI (Table 4). We specified a random effect for acquisition site. We covaried for age, sex, diagnosis, years of education, CSF t-tau, and *APOE*4 allele count. We also tested whether adding the sampling date difference between the date of CSF collection and the date of the MRI scan as a covariate in the statistical model modified the results. After adding sampling date difference as a covariate in the interaction analyses between CSF VEGF and CSF Aβ and t-tau on FDG-PET and cortical thickness, we did not find any difference in significant effects or interpretation. Therefore, we did not add sampling date difference in the statistical models for the reported findings. We used the false discovery rate (FDR) to correct for multiple comparisons (multiple ROIs).

Using the same mixed effects modeling strategy, we also evaluated whether continuous CSF t-tau and p-tau modified the association between VEGF and regional FDG-PET (Table 3) and cortical thickness (*Supplementary Table S2*). We added a product interaction term between VEGF and continuous CSF t-tau and p-tau (separately) on each FDG-PET and cortical thickness ROI and additionally covaried for continuous Aβ.

Table 2
Associations between VEGF levels and FDG-PET SUVR ROI analyzed in each Aβ stratum

	Aβ+ (n=116)				Aβ- (n=42)			
ROI	β	SE	p-value	FDR-adjusted p-value	β	SE	p-value	FDR-adjusted p-value
Superior Temporal Gyrus	0.15	0.08	0.065	0.15	-0.07	0.16	0.65	0.73
Middle Temporal Gyrus	0.25	0.09	0.006	0.027*	-0.15	0.19	0.44	0.73
Inferior Temporal Gyrus	0.26	0.09	0.003	0.027*	0.04	0.17	0.81	0.81
Fusiform Gyrus	0.11	0.09	0.19	0.22	0.09	0.16	0.57	0.73
Entorhinal Cortex	-0.05	0.08	0.48	0.48	0.10	0.16	0.52	0.73
Superior Parietal Cortex	0.17	0.12	0.15	0.22	-0.17	0.20	0.41	0.73
Inferior Parietal Cortex	0.32	0.12	0.009	0.027*	-0.18	0.22	0.42	0.73
Posterior Cingulate	0.16	0.11	0.17	0.22	-0.30	0.28	0.30	0.73
Precuneus	0.19	0.14	0.20	0.22	-0.17	0.26	0.52	0.73

Each association was evaluated using a linear mixed effects model. Fixed effects included CSF VEGF, age, sex, years of education, and CSF t-tau, *APOE*4, and diagnosis. Site was modeled using random effects. SE = Standard Error; FDR = False Discovery Rate.
* Indicates $p < 0.05$ significance

Table 3
Interactions between CSF VEGF levels and CSF t-tau and p-tau on FDG-PET ROIs (n=158)

	VEGF x t-tau				VEGF x p-tau			
ROI	β	SE	p-value	FDR-adjusted p-value	β	SE	p-value	FDR-adjusted p-value
Superior Temporal Gyrus	0.001	0.001	0.225	0.29	0.005	0.004	0.202	0.227
Middle Temporal Gyrus	0.003	0.001	0.008	0.037*	0.010	0.004	0.015	0.029*
Inferior Temporal Gyrus	0.003	0.001	0.028	0.051	0.011	0.004	0.010	0.029*
Fusiform Gyrus	0.0009	0.001	0.44	0.495	0.007	0.004	0.085	0.127
Entorhinal Cortex	-0.00003	0.001	0.97	0.97	0.004	0.004	0.270	0.270
Superior Parietal Cortex	0.003	0.001	0.026	0.051	0.013	0.005	0.009	0.029*
Inferior Parietal Cortex	0.004	0.002	0.008	0.037*	0.013	0.005	0.013	0.029*
Posterior Cingulate	0.003	0.002	0.067	0.10	0.008	0.006	0.153	0.197
Precuneus	0.004	0.002	0.028	0.051	0.016	0.006	0.016	0.029*

Each interaction term was evaluated using a linear mixed effects model. Fixed effects included CSF VEGF, age, sex, years of education, and CSF Aβ, *APOE*4, and diagnosis. Site was modeled using random effects. SE = Standard Error; FDR = False Discovery Rate.
* indicates $p < 0.05$ significance

Table 4
Associations between VEGF and cortical thickness ROI analyzed in each Aβ stratum

	Aβ+ (n=215)				Aβ- (n=95)			
ROI	β	SE	p-value	FDR-adjusted p-value	β	SE	p-value	FDR-adjusted p-value
Superior Temporal Gyrus	0.23	0.12	0.051	0.15	-0.35	0.15	0.028	0.062
Middle Temporal Gyrus	0.24	0.12	0.049	0.15	-0.23	0.15	0.13	0.17
Inferior Temporal Gyrus	0.20	0.12	0.098	0.22	-0.22	0.14	0.12	0.17
Fusiform Gyrus	0.23	0.12	0.051	0.15	-0.35	0.15	0.028	0.062
Entorhinal Cortex	0.46	0.34	0.18	0.29	-0.42	0.49	0.39	0.43
Superior Parietal Cortex	-0.09	0.10	0.39	0.44	-0.41	0.14	0.004	0.032*
Inferior Parietal Cortex	0.12	0.11	0.28	0.35	-0.34	0.14	0.021	0.062
Posterior Cingulate	0.13	0.10	0.19	0.29	-0.11	0.14	0.43	0.43
Precuneus	0.13	0.10	0.99	0.99	-0.20	0.12	0.10	0.17

Each association was evaluated using a linear mixed effects model. Fixed effects included VEGF, age, sex, years of education, and CSF t-tau, *APOE*4, and diagnosis. Site was modeled using random effects. FDR=False Discovery Rate. SE = Standard Error.
* Indicates $p < 0.05$ significance.

2.8.3. VEGF associations with cognitive measures: a secondary reproducibility analysis

We reproduced a cross-sectional analysis by Hohman et al. 2015 in a similar ADNI dataset and expanded on the analysis. We reproduced the interaction analysis between VEGF and continuous Aβ on ADNI-EF and ADNI-MEM, but also evaluated whether an association would be detected when stratified by Aβ-positivity. We used a linear mixed effects model (covarying for age, sex, diagnosis, years of education, CSF t-tau, and *APOE*4 allele count) and included random effects for acquisition site. This statistical approach varied slightly from that used in Hohman et al.; Hohman et al. 2015 used a general linear model to test associations, whereas we additionally covaried for site, *APOE*4 allele count, as well as CSF t-tau and continuous Aβ in the interaction analyses.

We expanded upon the analysis and addressed limitations of the cognitive composite measures tested by evaluating associations between VEGF and each subtest incorporated in the composite measure. Since associations were only significant at the composite level (ADNI-EF) in the Aβ+, but not the Aβ- stratum, we used a linear mixed effects model to correlate VEGF with each ADNI-EF composite measure subtest in the Aβ+ stratum. Each neuropsychological subtest that comprised the cognitive composite measure was Z-score transformed using the entire cohort (N=310) to obtain the mean and SD for the transformation. In neuropsychological subtests that are binary (e.g., clock drawing items), we performed logistic regression using a generalized linear mixed effects model with a logit link function.

Table 5
Regional mediation effects in Aβ+ participants (n=116)

Mediational Process	Inferior Temporal Gyrus			Middle Temporal Gyrus			Inferior Parietal Cortex		
	β	95% CI	p-value	β	95% CI	p-value	β	95% CI	p-value
CSF VEGF → FDG-PET SUVR ROI → ADNI-EF									
Indirect effect	0.54	(0.14, 1.08)	0.006*	0.35	(0.05, 0.78)	0.016*	0.59	(0.14, 1.22)	0.010*
Direct effect	1.11	(-0.03, 2.16)	0.060	1.25	(0.16, 2.41)	0.026*	1.07	(0.07, 2.12)	0.036*
Total effect	1.65	(0.51, 2.73)	0.002*	1.60	(0.48, 2.80)	0.006*	1.66	(0.59, 2.84)	0.002*
Proportion Mediated	0.33	(0.09, 1.05)	0.008*	0.21	(0.03, 0.70)	0.022*	0.36	(0.10, 0.90)	0.012*

ROI = Region of Interest.
* $p < 0.05$ significance

2.8.4. Mediation analysis

We performed mediation analyses to evaluate the direct and indirect associations between VEGF and cognition in Aβ+ participants. We evaluated the extent to which the previously reported association between VEGF and ADNI-EF was direct or mediated by regional FDG-PET SUVR. We performed three causal mediation analyses (Table 5) across the three regions (inferior parietal cortex, MTG and ITG) in which we found a significant relationship between VEGF levels and FDG-PET signal in Aβ+ participants. The R package mediation 4.4.6 (simulations = 1000) was used to perform all analyses.

3. Results

3.1. Relationship between VEGF and Aβ levels

A summary of participant characteristics in the entire cohort (N = 310) and separately in Aβ+ (n = 215) and Aβ- (n = 95) stratum can be found in Table 1, where we also compared amyloid group (Aβ+ vs. Aβ-) differences in these variables. Differences between groups were found in diagnosis and *APOE*4 allele count and Aβ+ individuals had significantly lower VEGF levels, lower MMSE scores, and higher t-tau and p-tau levels than Aβ- individuals (Table 1). In a separate analysis of CSF VEGF levels by AD neuropathology load, individuals who were Aβ+ and t-tau- (n = 91) had significantly lower VEGF levels than those who were both Aβ- and t-tau- (n = 86; $p < 0.001$) and those who were both Aβ+ and t-tau+ (n = 124, $p < 0.001$) (*Supplementary Figure S1*). VEGF levels did not differ between the Aβ- t-tau- and Aβ+ t-tau+ groups. We also evaluated the association between continuous CSF Aβ levels (using a piecewise linear mixed effects spline model with a knot at 192 pg/mL; cutoff for Aβ-positivity) and VEGF. The full table of statistical associations can be found in the *Supplementary Table S1*. Briefly, older age, MCI diagnosis, male sex, higher CSF t-tau, and greater CSF Aβ levels in both individuals with Aβ < 192 pg/mL (Aβ+) and in those with Aβ > 192 pg/mL (Aβ-) were associated with higher VEGF levels.

3.2. VEGF associations with regional FDG-PET SUVR

All associations between VEGF levels and FDG-PET ROIs by Aβ stratum are in Table 2. In Aβ+ participants (n = 116), higher VEGF levels were associated with a higher mean bilateral FDG-PET signal in the inferior parietal cortex (VEGF partial β (SE) = 0.32 (0.12); FDR-adjusted $p = 0.027$), MTG (VEGF partial β (SE) = 0.25 (0.09); FDR-adjusted $p = 0.027$), and ITG (VEGF partial β (SE) = 0.26 (0.09); FDR-adjusted $p = 0.027$). No significant association between VEGF levels and FDG-PET SUVR ROIs were found in Aβ- participants (n = 42). The beta-estimates between Aβ+ and Aβ- participants were significantly different in the posterior cingulate cortex (FDR interaction $p = 0.0496$), but no other region had a significant interactive effect that passed FDR correction (FDR interaction p-values > 0.21).

We evaluated interaction effects between VEGF and CSF t-tau and p-tau on regional FDG-PET SUVR (**Table 3**). After FDR correction, interactions between VEGF and t-tau and VEGF and p-tau were both significant in the MTG and inferior parietal cortex (FDR-adjusted p-values < 0.037). The ITG, superior parietal cortex, and precuneus also were regions to have significant interactions between VEGF and p-tau (all FDR-adjusted p-values = 0.029) and trend level interactions between VEGF and t-tau (all FDR-adjusted p-values = 0.051), where those with higher levels of tau had a stronger positive association between VEGF and regional FDG-PET SUVR than those with lower tau. **Figure 2** illustrates plots of interactions between VEGF levels and CSF Aβ, t-tau, and p-tau on FDG-PET SUVR in the inferior parietal, MTG, and ITG.

3.3. VEGF associations with regional cortical thickness

In Aβ+ participants, higher VEGF levels were nominally associated with greater MTG cortical thickness (VEGF partial β (SE) = 0.24 (0.12); $p = 0.049$), but after FDR correction VEGF was not associated with any cortical thickness ROI in Aβ+ participants. In Aβ- participants, higher VEGF was associated with a thinner superior parietal cortex (VEGF partial β (SE) = -0.41 (0.14); FDR-adjusted $p = 0.032$) and trend level associated with a thinner cortex in the STG, fusiform, and inferior parietal cortex (all regions VEGF FDR-adjusted partial $p = 0.062$). The beta-estimates nominally differed between Aβ+ and Aβ- participants in the MTG (interaction $p = 0.031$) and superior parietal cortex (interaction $p = 0.015$), but did not pass FDR correction (FDR-adjusted interaction p-values = 0.14). No significant interactions between VEGF and t-tau or p-tau were found on cortical thickness ROIs (*Supplementary Table S2*).

3.4. VEGF associations with cognitive measures: A secondary reproducibility analysis

Hohman et al., found that higher VEGF levels (in an interaction analysis with continuous CSF Aβ and t-tau) were not associated with baseline ADNI-EF or ADNI-MEM, but were associated with less ADNI-EF and ADNI-MEM longitudinal decline. In our reproduction of the Hohman et al. 2015 baseline cross-sectional analysis between VEGF and ADNI-EF and ADNI-MEM, we found similar negative results that neuropathological hallmarks do not interact with VEGF on ADNI-EF (Aβ interaction $p = 0.65$; t-tau interaction $p = 0.43$) and ADNI-MEM (Aβ interaction $p = 0.45$; t-tau interaction $p = 0.09$). When we ran the analysis without an interaction term, we found that higher VEGF levels were associated with greater ADNI-EF (VEGF partial β (SE) = 1.14 (0.38); FDR-adjusted $p = 0.006$) and ADNI-MEM scores (VEGF partial β (SE) = 0.67 (0.30); FDR-adjusted $p = 0.026$), whereas Hohman et al. did not find a main effect of VEGF on composite mea-

sures cross-sectionally. In our stratum-specific analysis, we found in Aβ+ participants only (n = 215), higher VEGF levels were significantly associated with better ADNI-EF scores (CSF VEGF partial β (SE) = 1.19 (0.49); FDR-adjusted $p = 0.031$). The association between VEGF levels and ADNI-MEM in Aβ+ participants had trend-level significance (VEGF partial β (SE) = 0.67 (0.37); FDR-adjusted $p = 0.070$). In Aβ- participants, VEGF was not related to ADNI-EF (VEGF partial β (SE) = 0.29 (0.61); FDR-adjusted $p = 0.635$) or ADNI-MEM (VEGF partial β (SE) = 0.59 (0.56); FDR-adjusted $p = 0.593$). Although the effect size for the association of VEGF to ADNI-EF was larger in the Aβ+ stratum than in the Aβ- stratum, this difference was not significant (interaction p-value = 0.22). The sample size of the Aβ- stratum was significantly smaller than the Aβ+ stratum and therefore, we may be underpowered to detect a true interaction if one exists.

To further address limitations of domain specific cognitive measures and evaluate cognitive components driving the association between VEGF and executive function in Aβ+ participants, we evaluated the relationship between VEGF and each of the neuropsychological tests that comprise the ADNI-EF composite score in Aβ participants. Higher VEGF levels were associated with better Category Fluency – vegetables (VEGF partial β (SE) = 1.90 (0.52); $p < 0.001$) and Category Fluency – animals scores (VEGF partial β (SE) = 1.28 (0.53); $p = 0.018$). No other ADNI-EF subtests were associated with VEGF levels (*Supplementary Table S3*).

3.5. Mediation analysis

We next evaluated whether the association between VEGF and ADNI-EF was direct or mediated by regional FDG-PET signal. We focused only on those regions in which we found a significant relationship between VEGF and FDG-PET signal: mean bilateral ITG, MTG, and inferior parietal cortex (Table 5). We found that FDG-PET signal in all three regions mediated the relationship between VEGF and ADNI-EF.

4. Discussion

Our study evaluated the relationship between CSF VEGF levels and regional glucose metabolism and cortical thickness by evaluating whether relationships were modified by CSF Aβ, t-tau, and p-tau levels. We also evaluated whether regional FDG-PET signal mediates an association between VEGF and cognition. Our results revealed that 1) VEGF has regionally-specific structural and metabolic associations in AD-signature regions, particularly in lateral temporal-parietal cortices, 2) the association between VEGF and FDG-PET ROIs was stronger in those with abnormal levels of AD neuropathology (CSF Aβ, t-tau and p-tau), 3) in Aβ+ individuals, higher VEGF levels were associated with better scores on temporal-mediated language measures (i.e., category fluency) and 4) VEGF had both a direct relationship with cognitive function in individuals along the AD continuum and an indirect relationship, mediated by regional FDG-PET signal.

In Aβ+ participants, higher VEGF levels were associated with greater mean bilateral glucose metabolism in the inferior parietal cortex, and in the middle and inferior temporal gyri, which were also regions that exhibited an interactive effect between VEGF and t-tau and p-tau. Previous work in the same cohort that only evaluated the association between VEGF and global FDG-PET SUVR (but not regional indices) found a similar direction of association (Wang et al., 2018). This work also aligns with other studies demonstrating that AD-related pathology is preferentially associated with regional decreases in FDG-PET SUVR and cortical thickness in the lateral temporal regions (Dowling et al., 2015; Malpas et al., 2018). The temporal lobe may be more vulnerable to hypometabolism because it is preferentially impacted by early Aβ accumulation (Braak and Braak, 1991) and reduced VEGF expression, as seen in post-mortem AD brains with high amyloid plaque load (Provias and Jeynes, 2014). However, the regions in which we found significant associations do not align exclusively with the spatial trajectory of AD-associated neuropathology. Therefore, other vascular factors may contribute to the spatial specificity of VEGF, warranting further investigation. For example, lower cerebral blood flow (CBF) and higher CSF soluble platelet-derived growth factor (i.e., measures of vascular function) have been recently associated with greater tau PET burden in similar temporo-parietal regions to those found in our study, suggesting that these regions are particularly vulnerable to vascular interactions with AD neuropathology (Albrecht et al., 2020). Also, the inferior parietal, middle and inferior temporal gyri comprise vascular territory watershed regions, which are susceptible to hypoperfusion in AD (Huang et al., 2018). Future work should evaluate these potential mechanisms driving the topographical correspondence of VEGF levels.

Our identified positive associations between VEGF levels and FDG-PET signal could also represent a response to early blood brain barrier (BBB) damage, where VEGF levels increase to help restore BBB's glucose transporter-1 (GLUT1) levels (which are responsible for carrying FDG across the BBB in FDG-PET scanning of the brain). Evidence of this compensatory relationship has been seen in animal models, where GLUT1 levels decrease in response to a high fat diet, which results in a compensatory increase in VEGF expression to help restore BBB vascular endothelial cell GLUT1 levels, glucose uptake and cognitive function (Jais et al., 2016). Further, FDG-PET signal reductions could also be more representative of impaired GLUT1-faciliated BBB transport (i.e., vascular dysfunction) than glucose metabolism, since FDG does not get metabolized by downstream metabolic pathways and only tracks glucose transport shortly after brain uptake (Sweeney et al., 2019).

The direction and strength of the relationship between VEGF and AD brain biomarkers varied by AD-neuropathological marker abnormality. Higher VEGF levels were associated with greater regional FDG-PET SUVR and nominally related to a thicker cortex in Aβ+ participants, possibly representing a neuroprotective effect of VEGF. Although the relationship between VEGF and cortical thickness has not been evaluated previously, other measures of vascular dysfunction (e.g., capillary mean transit time, CSF vascular adhesion molecule-1, CSF intercellular adhesion molecule-1) have been associated with temporo-parietal cortical thinning and worse cognition (Janelidze et al., 2018; Nielsen et al., 2017), consistent with Aβ+ group findings. We also found a significant interaction between VEGF and CSF t-tau and p-tau on regional FDG-PET, where higher levels of tau strengthened the positive association between VEGF and FDG-PET, even after adjusting for amyloid. While both t-tau and p-tau had interactive effects with VEGF on FDG-PET SUVR in the MTG and inferior parietal cortex, p-tau also modified the association between VEGF and FDG-PET in the ITG, superior parietal cortex and precuneus. This may reflect more of an interaction between vascular dysfunction and tau phosphorylation (i.e., p-tau) early in the AD cascade (particularly in watershed regions that are vulnerable to vascular deficits), rather than later after neurodegeneration (reflected by t-tau levels) has begun (Blennow et al., 2010). These results also suggest that Aβ and tau have independent effects on the relationship between VEGF and FDG-PET. However, as a cross-sectional study, we cannot determine whether VEGF, amyloid, or tau is modifying the relationship with FDG-PET.

In Aβ- participants, VEGF levels were not related to regional FDG-PET SUVR and higher VEGF was associated with a thinner superior parietal cortex. This unexpected finding may suggest that higher VEGF levels (when amyloid levels are minimal) signal an injury response driven by something other than AD-neuropathology.

For instance, injury could result from dysfunctional vascular and metabolic processes that promote inflammation, vessel permeability, leakage and neuronal loss (Van Dyken and Lacoste, 2018). Variability in the directionality of the findings may also be related to possible interactive effects between Aβ and tau on VEGF levels. In our group analysis of VEGF levels, individuals with the lowest (Aβ- and t-tau-) and highest (Aβ+ and t-tau+) neuropathological burden had significantly higher VEGF levels than those who were only Aβ+ (and t-tau-), which may reflect a U-shaped trajectory of VEGF levels in AD pathogenesis. However, as a cross-sectional study we cannot evaluate these mechanisms formally.

In our reproducibility analysis of the interaction between VEGF and CSF Aβ on cognitive domain measures, we did not find a significant interaction between VEGF and Aβ on ADNI-EF and ADNI-MEM composite measures - similar to Hohman et al. 2015. However, in our Aβ stratified analysis, we found that higher VEGF levels were associated with better ADNI-EF scores. We may have found this cross-sectional association between VEGF and ADNI-EF because 1) differences in the sample size of the Aβ stratums may mask a formal interaction if a true one exists, and 2) we also adjusted for CSF t-tau levels, *APOE4* genotype, and acquisition site in our statistical model. The executive function measure we used (ADNI-EF) is a heterogeneous construct that actually includes both tests of executive function and language. Our subtest analysis revealed that the association between higher VEGF levels and higher ADNI-EF was driven by category fluency (vegetables and animals) scores. Although category fluency tasks have a generation component, they are typically considered measures of language and semantic knowledge, not executive function measures *per se*. This finding may reflect changes in temporal lobe-mediated language function (rather than frontal-mediated EF), and suggests that VEGF may have an effect on temporal lobe function independent of tau (which we controlled for in our analysis). While few studies have correlated VEGF with different cognitive measures, a multi-cohort study in AD and cognitively intact participants found that individuals with better cognitive (MMSE) scores had higher VEGF levels (Leung et al., 2015), a similar direction of effect we found in our study.

VEGF had both direct effects on ADNI-EF scores, and also indirect effects, mediated by regional FDG-PET signal. Past studies have reported comparable findings; regional temporal lobe FDG-PET hypometabolism was associated with EF in AD (Habeck et al., 2012) and also mediated the association between baseline AD CSF biomarkers and subsequent cognitive decline (Dowling et al., 2015). The regional specificity of FDG-PET on ADNI-EF may be driven by verbal fluency, as the measure recruits both frontal and temporal lobe brain regions (Melrose et al., 2009). Particularly, worse performance on category naming tests and retrieval of semantic knowledge is associated with region-specific metabolic decreases in the inferior temporal lobes (Melrose et al., 2009), a region we also identified to be associated with VEGF. Our findings could also be attributed to disruption of more global structural cortical connections, such as between the frontal and temporal lobes (Wiseman et al., 2015). The presence of both direct and indirect associations suggests that multiple AD brain biomarkers and pathways contribute to cognitive impairment.

Future work should evaluate the temporal and spatial correspondence between VEGF levels and AD brain biomarkers, and further integrate complex models and interactions in larger samples that can address the multitude of factors (e.g., inflammation, atherosclerosis) that modify VEGF signaling. Our study has some limitations. First, we included VEGF levels acquired at only one time point. VEGF levels may fluctuate from the time of CSF collection to the time of the brain scans and neuropsychological testing. We also cannot directly evaluate whether VEGF is upregulated and therefore cannot infer directionality or causality of the relationships. Although we had *a priori* hypotheses regarding the temporal ordering of variables used in the mediation analysis, future work would benefit from longitudinal analysis to assess mediation effects. Additionally, the spatial specificity of amyloid and VEGF in the brain is also unknown, since both variables were assessed by a global CSF measure. Sample sizes after stratifying FDG-PET participants were also small, particularly in the Aβ- stratum, limiting our statistical power to formally detect interaction effects. Since samples were also uneven in sex (females < males) and diagnostic groups (AD < CI < MCI), future large-scale initiatives should aim to balance sex and diagnostic group sample sizes. Despite these limitations, this study is the largest study-to-date evaluating regional relationships between CSF VEGF and AD brain biomarkers. Further, this study is an important step in evaluating mechanisms and populations most at-risk for suboptimal brain aging.

Our study helps clarify the relationship between endogenous CSF VEGF and Aβ in humans and expands on previously detected associations between VEGF and cognition (Hohman et al., 2015) and global FDG-PET (Wang et al., 2018) by 1) identifying regional relationships between VEGF and FDG-PET and cortical thickness – indices that are altered early in AD pathogenesis and provide spatial specificity to heterogeneity in AD, and 2) assessing whether the association between VEGF and cognition was mediated by FDG-PET signal. Our results suggest that at different amyloid and tau loads, there is variability in the relationship between VEGF and regionally specific brain measures. Higher endogenous VEGF levels may signal a vascular injury response when AD-neuropathological load is low, but serve a compensatory neuroprotective role when AD-neuropathological burden is high. VEGF may also serve as a valuable biomarker in understanding vascular and metabolic contributions to variability in AD neuroimaging phenotypes. Lastly, VEGF is modifiable, such as through exercise (Viboolvorakul and Patumraj, 2014), making it a potentially therapeutic target in AD and warranting future investigation on its contribution to modulating AD risk.

Verification

We have not published these results elsewhere, including on the internet, nor is this paper under consideration for publication elsewhere. The publication has been approved by all authors.

Acknowledgement

This work was supported in part by NIH grants T32 MH111360 (Levitt), F31 AG059356 (Tubi), R01 AG041915 (Thompson), and P50 AG05142 (Chui), R01 AG054073 (Sid O'Bryant), R01 AG058162 (Chui, Marmarelis, Billinger, Zhang), and P01 AG055367 (Chen & Finch). Data collection and sharing for this project was funded by the Alzheimer's Disease Neuroimaging Initiative (ADNI) (National Institutes of Health Grant U01 AG024904) and DOD ADNI (Department of Defense award number W81XWH-12-2-0012). ADNI is funded by the National Institute of Biomedical Imaging and Bioengineering, the National Institute on Aging, and through generous support from the following: AbbVie, Alzheimer's Association; Alzheimer's Drug Discovery Foundation; Araclon Biotech; BioClinica, Inc.; Biogen; Bristol-Myers Squibb Company; CereSpir, Inc.; Cogstate; Eisai Inc.; Elan Pharmaceuticals, Inc.; Eli Lilly and Company; EuroImmun; F. Hoffmann-La Roche Ltd and its affiliated company Genentech, Inc.; Fujirebio; GE Healthcare; IXICO Ltd.; Janssen Alzheimer Immunotherapy Research & Development, LLC.; Johnson & Johnson Pharmaceutical Research & Development LLC.; Lumosity; Lundbeck; Merck & Co., Inc.; Meso Scale

Diagnostics, LLC.; NeuroRx Research; Neurotrack Technologies; Novartis Pharmaceuticals Corporation; Pfizer Inc.; Piramal Imaging; Servier; Takeda Pharmaceutical Company; and Transition Therapeutics. The Canadian Institutes of Health Research contributes to support ADNI clinical sites in Canada. Private sector resources are coordinated by the Foundation for the National Institutes of Health (www.fnih.org). The grantee organization is the Northern California Institute for Research and Education, and the study is organized by the Alzheimer's Therapeutic Research Institute at the University of Southern California. ADNI data are distributed by the Laboratory for Neuro Imaging at the University of Southern California.

Supplementary materials

Supplementary material associated with this article can be found, in the online version, at doi:10.1016/j.neurobiolaging.2021.04.025.

CRediT authorship contribution statement

Meral A. Tubi: Conceptualization, Methodology, Formal analysis, Writing – original draft, Investigation, Software, Funding acquisition. **Deydeep Kothapalli:** Investigation, Visualization, Software. **Matthew Hapenney:** Investigation, Software. **Wendy J. Mack:** Writing – review & editing, Methodology. **Kevin S. King:** Writing – review & editing. **Paul M. Thompson:** Supervision, Funding acquisition, Writing – review & editing, Resources. **Meredith N. Braskie:** Supervision, Funding acquisition, Writing – review & editing, Conceptualization, Methodology, Resources.

References

Albrecht, D., Isenberg, A.L., Stradford, J., Monreal, T., Sagare, A., Pachicano, M., Sweeney, M., Toga, A., Zlokovic, B., Chui, H., Joe, E., Schneider, L., Conti, P., Jann, K., Pa, J., 2020. Associations between Vascular Function and Tau PET Are Associated with Global Cognition and Amyloid. J Neurosci 40 (44), 8573–8586.

Angom, S., Wang, Y., Wang, E., Pal, K., Bhattacharya, S., Watzlawik, J.O., Rosenberry, T.L., Das, P., Mukhopadhyay, D., 2019. VEGF receptor-1 modulates amyloid beta 1-42 oligomer-induced senescence in brain endothelial cells. Faseb j 33 (3), 4626–4637.

Avants, B.B., Epstein, C.L., Grossman, M., Gee, J.C., 2008. Symmetric diffeomorphic image registration with cross-correlation: evaluating automated labeling of elderly and neurodegenerative brain. Med Image Anal 12 (1), 26–41.

Avants, B.B., Tustison, N.J., Song, G., Cook, P.A., Klein, A., Gee, J.C., 2011. A reproducible evaluation of ANTs similarity metric performance in brain image registration. Neuroimage 54 (3), 2033–2044.

Bennett, R.E., Robbins, A.B., Hu, M., Cao, X., Betensky, R.A., Clark, T., Das, S., Hyman, B.T., 2018. Tau induces blood vessel abnormalities and angiogenesis-related gene expression in P301L transgenic mice and human Alzheimer's disease. Proc Natl Acad Sci U S A 115 (6), E1289–E1298.

Blennow, K., Hampel, H., Weiner, M., Zetterberg, H., 2010. Cerebrospinal fluid and plasma biomarkers in Alzheimer disease. Nat Rev Neurol 6 (3), 131–144.

Box, G.E.P., Cox, D.R., 1964. An analysis of transformations. Journal of the Royal Statistical Society 26 (2), 211–252.

Makkar, SR, Lipnicki, DM, Crawford, JD, Kochan, NA, Castro-Costa, E, Lima-Costa, MF, Diniz, BS, Brayne, C, Stephan, B, Matthews, F, Llibre-Rodriguez, JJ, Llibre-Guerra, JJ, Valhuerdi-Cepero, AJ, Lipton, RB, Katz, MJ, Wang, C, Ritchie, K, Carles, S, Carriere, I, Scarmeas, N, Yannakoulia, M, Kosmidis, M, Lam, L, Chan, WC, Fung, A, Guaita, A, Vaccaro, R, Davin, A, Kim, KW, Han, JW, Suh, SW, Riedel-Heller, SG, Roehr, S, Pabst, A, Ganguli, M, Hughes, TF, Snitz, B, Anstey, KJ, Cherbuin, N, Easteal, S, Haan, MN, Aiello, AE, Dang, K, Pin Ng, T, Gao, Q, Zin Nyunt, MS, Brodaty, H, Trollor, JN, Leung, Y, Lo, JW, Sachdev, P, 2020. APOE ε4 and the Influence of Sex, Age, Vascular Risk Factors, and Ethnicity on Cognitive Decline. J Gerontol A Biol Sci Med Sci. 75 (10), 1863–1873. doi:10.1093/gerona/glaa116, Sep 25PMID: 32396611; PMCID: PMC7518559.

Braak, H., Braak, E., 1991. Neuropathological stageing of Alzheimer-related changes. Acta Neuropathol (Berl) 82 (4), 239–259.

Braskie, M.N., Boyle, C.P., Rajagopalan, P., Gutman, B.A., Toga, A.W., Raji, C.A., Tracy, R.P., Kuller, L.H., Becker, J.T., Lopez, O.L., Thompson, P.M., 2014. Physical activity, inflammation, and volume of the aging brain. Neuroscience 273, 199–209.

Burggren, A.C., Zeineh, M.M., Ekstrom, A.D., Braskie, M.N., Thompson, P.M., Small, G.W., Bookheimer, S.Y., 2008. Reduced cortical thickness in hippocampal subregions among cognitively normal apolipoprotein E e4 carriers. Neuroimage 41 (4), 1177–1183.

Cao, L., Jiao, X., Zuzga, D.S., Liu, Y., Fong, D.M., Young, D., During, M.J., 2004. VEGF links hippocampal activity with neurogenesis, learning and memory. Nat Genet 36 (8), 827–835.

Chakraborty, A., Chatterjee, M., Twaalfhoven, H., Del Campo Milan, M., Teunissen, C.E., Scheltens, P., Fontijn, R.D., van Der Flier, W.M., de Vries, H.E., 2018. Vascular Endothelial Growth Factor remains unchanged in cerebrospinal fluid of patients with Alzheimer's disease and vascular dementia. Alzheimers Res Ther 10 (1), 58.

Cho, S.J., Park, M.H., Han, C., Yoon, K., Koh, Y.H., 2017. VEGFR2 alteration in Alzheimer's disease. Sci Rep 7 (1), 17713.

Crane, P.K., Carle, A., Gibbons, L.E., Insel, P., Mackin, R.S., Gross, A., Jones, R.N., Mukherjee, S., Curtis, S.M., Harvey, D., Weiner, M., Mungas, D.Alzheimer's Disease Neuroimaging, I., 2012. Development and assessment of a composite score for memory in the Alzheimer's Disease Neuroimaging Initiative (ADNI). Brain Imaging Behav 6 (4), 502–516.

Dale, A.M., Fischl, B., Sereno, M.I., 1999. Cortical Surface-Based Analysis.pdf. NeuroImage 9, 179–194.

Dowling, N.M., Johnson, S.C., Gleason, C.E., Jagust, W.J.Alzheimer's Disease Neuroimaging, I., 2015. The mediational effects of FDG hypometabolism on the association between cerebrospinal fluid biomarkers and neurocognitive function. Neuroimage 105, 357–368.

Fischl, B., Dale, A.M., 2000. Measuring the thickness of the human cerebral cortex from magnetic resonance images. Proc Natl Acad Sci U S A 97 (20), 11050–11055.

Fournier, N.M., Lee, B., Banasr, M., Elsayed, M., Duman, R.S., 2012. Vascular endothelial growth factor regulates adult hippocampal cell proliferation through MEK/ERK- and PI3K/Akt-dependent signaling. Neuropharmacology 63 (4), 642–652.

Gibbons, L.E., Carle, A.C., Mackin, R.S., Harvey, D., Mukherjee, S., Insel, P., Curtis, S.M., Mungas, D., Crane, P.K.Alzheimer's Disease Neuroimaging, I., 2012. A composite score for executive functioning, validated in Alzheimer's Disease Neuroimaging Initiative (ADNI) participants with baseline mild cognitive impairment. Brain Imaging Behav 6 (4), 517–527.

Gora-Kupilas, K., Josko, J., 2005. The neuroprotective function of vascular endothelial growth factor (VEGF). Folia Neuropathol 43 (1), 31–39.

Habeck, C., Risacher, S., Lee, G.J., Glymour, M.M., Mormino, E., Mukherjee, S., Kim, S., Nho, K., DeCarli, C., Saykin, A.J., Crane, P.K., 2012. Relationship between baseline brain metabolism measured using [(1)(8)F]FDG PET and memory and executive function in prodromal and early Alzheimer's disease. Brain Imaging Behav 6 (4), 568–583.

Hedden, T., Oh, H., Younger, A.P., Patel, T.A., 2013. Meta-analysis of amyloid-cognition relations in cognitively normal older adults. Neurology 80 (14), 1341–1348.

McKhann, G, Drachman, D, Folstein, M, Katzman, R, Price, D, Stadlan, EM., 1984. Clinical diagnosis of Alzheimer's disease: report of the NINCDS-ADRDA Work Group under the auspices of Department of Health and Human Services Task Force on Alzheimer's Disease. Neurology 34 (7), 939–944. doi:10.1212/wnl.34.7.939, JulPMID: 6610841.

Hobel, Z, Isenberg, AL, Raghupathy, D, Mack, W, Pa, JAlzheimer's Disease Neuroimaging Initiative and the Australian Imaging Biomarkers and Lifestyle flagship study of ageing, 2019. APOEε4 Gene Dose and Sex Effects on Alzheimer's Disease MRI Biomarkers in Older Adults with Mild Cognitive Impairment. J Alzheimers Dis 71 (2), 647–658. doi:10.3233/JAD-180859.

Hohman, T.J., Bell, S.P., Jefferson, A.L.Alzheimer's Disease Neuroimaging, I., 2015. The role of vascular endothelial growth factor in neurodegeneration and cognitive decline: exploring interactions with biomarkers of Alzheimer disease. JAMA Neurol 72 (5), 520–529.

Holtzman, D.M., 2011. CSF biomarkers for Alzheimer's disease: current utility and potential future use. Neurobiol Aging 32 (Suppl 1), S4–S9.

Huang, C.W., Hsu, S.W., Chang, Y.T., Huang, S.H., Huang, Y.C., Lee, C.C., Chang, W.N., Lui, C.C., Chen, N.C., Chang, C.C., 2018. Cerebral Perfusion Insufficiency and Relationships with Cognitive Deficits in Alzheimer's Disease: A Multiparametric Neuroimaging Study. Sci Rep 8 (1), 1541.

Jack Jr., C.R., Holtzman, D.M., 2013. Biomarker modeling of Alzheimer's disease. Neuron 80 (6), 1347–1358.

Jagust, W.J., Bandy, D., Chen, K., Foster, N.L., Landau, S.M., Mathis, C.A., Price, J.C., Reiman, E.M., Skovronsky, D., Koeppe, R.A.Alzheimer's Disease Neuroimaging, I., 2010. The Alzheimer's Disease Neuroimaging Initiative positron emission tomography core. Alzheimers Dement 6 (3), 221–229.

Jais, A., Solas, M., Backes, H., Chaurasia, B., Kleinridders, A., Theurich, S., Mauer, J., Steculorum, S.M., Hampel, B., Goldau, J., Alber, J., Forster, C.Y., Eming, S.A., Schwaninger, M., Ferrara, N., Karsenty, G., Bruning, J.C., 2016. Myeloid-Cell-Derived VEGF Maintains Brain Glucose Uptake and Limits Cognitive Impairment in Obesity. Cell 165 (4), 882–895.

Janelidze, S., Mattsson, N., Stomrud, E., Lindberg, O., Palmqvist, S., Zetterberg, H., Blennow, K., Hansson, O., 2018. CSF biomarkers of neuroinflammation and cerebrovascular dysfunction in early Alzheimer disease. Neurology 91 (9), e867–e877.

Joshi, A., Koeppe, R.A., Fessler, J.A., 2009. Reducing between scanner differences in multi-center PET studies. Neuroimage 46 (1), 154–159.

Jurado, M.B., Rosselli, M., 2007. The elusive nature of executive functions: a review of our current understanding. Neuropsychol Rev 17 (3), 213–233.

Landau, S.M., Mintun, M.A., Joshi, A.D., Koeppe, R.A., Petersen, R.C., Aisen, P.S., Weiner, M.W., Jagust, W.J.Alzheimer's Disease Neuroimaging, I., 2012. Amyloid deposition, hypometabolism, and longitudinal cognitive decline. Ann Neurol 72 (4), 578–586.

Jenkinson, M, Smith, S., 2001 Jun. A global optimisation method for robust affine registration of brain images. Med Image Anal 5 (2), 143–156. doi:10.1016/s1361-8415(01)00036-6, PMID: 11516708.

Jenkinson, M, Bannister, P, Brady, M, Smith, S., 2002. Improved optimization for the robust and accurate linear registration and motion correction of brain images. Neuroimage 17 (2), 825–841. doi:10.1016/s1053-8119(02)91132-8, OctPMID: 12377157.

Lange, C., Storkebaum, E., de Almodovar, C.R., Dewerchin, M., Carmeliet, P., 2016. Vascular endothelial growth factor: a neurovascular target in neurological diseases. Nat Rev Neurol 12 (8), 439–454.

Leung, Y.Y., Toledo, J.B., Nefedov, A., Polikar, R., Raghavan, N., Xie, S.X., Farnum, M., Schultz, T., Baek, Y., Deerlin, V.V., Hu, W.T., Holtzman, D.M., Fagan, A.M., Perrin, R.J., Grossman, M., Soares, H.D., Kling, M.A., Mailman, M., Arnold, S.E., Narayan, V.A., Lee, V.M., Shaw, L.M., Baker, D., Wittenberg, G.M., Trojanowski, J.Q., Wang, L.S., 2015. Identifying amyloid pathology-related cerebrospinal fluid biomarkers for Alzheimer's disease in a multicohort study. Alzheimers Dement (Amst) 1 (3), 339–348.

Licht, T., Goshen, I., Avital, A., Kreisel, T., Zubedat, S., Eavri, R., Segal, M., Yirmiya, R., Keshet, E., 2011. Reversible modulations of neuronal plasticity by VEGF. Proc Natl Acad Sci U S A 108 (12), 5081–5086.

Malpas, C.B., Saling, M.M., Velakoulis, D., Desmond, P., Hicks, R.J., Zetterberg, H., Blennow, K., O'Brien, T.J., 2018. Cerebrospinal Fluid Biomarkers are Differentially Related to Structural and Functional Changes in Dementia of the Alzheimer's Type. J Alzheimers Dis 62 (1), 417–427.

Melrose, R.J., Campa, O.M., Harwood, D.G., Osato, S., Mandelkern, M.A., Sultzer, D.L., 2009. The neural correlates of naming and fluency deficits in Alzheimer's disease: an FDG-PET study. Int J Geriatr Psychiatry 24 (8), 885–893.

Nielsen, R.B., Egefjord, L., Angleys, H., Mouridsen, K., Gejl, M., Moller, A., Brock, B., Braendgaard, H., Gottrup, H., Rungby, J., Eskildsen, S.F., Ostergaard, L., 2017. Capillary dysfunction is associated with symptom severity and neurodegeneration in Alzheimer's disease. Alzheimers Dement.

Ossenkoppele, R., Smith, R., Ohlsson, T., Strandberg, O., Mattsson, N., Insel, P.S., Palmqvist, S., Hansson, O., 2019. Associations between tau, Aβ, and cortical thickness with cognition in Alzheimer disease. Neurology 92 (6), e601–e612.

Paterson, R.W., Bartlett, J.W., Blennow, K., Fox, N.C., Shaw, L.M., Trojanowski, J.Q., Zetterberg, H., Schott, J.M.Alzheimer's Disease Neuroimaging, I, 2014. Cerebrospinal fluid markers including trefoil factor 3 are associated with neurodegeneration in amyloid-positive individuals. Transl Psychiatry 4, e419.

Provias, J., Jeynes, B., 2014. Reduction in vascular endothelial growth factor expression in the superior temporal, hippocampal, and brainstem regions in Alzheimer's disease. Curr Neurovasc Res 11 (3), 202–209.

Querbes, O., Aubry, F., Pariente, J., Lotterie, J.A., Demonet, J.F., Duret, V., Puel, M., Berry, I., Fort, J.C., Celsis, P.Alzheimer's Disease Neuroimaging, I., 2009. Early diagnosis of Alzheimer's disease using cortical thickness: impact of cognitive reserve. Brain 132 (Pt 8), 2036–2047.

R Core Development Team, 2010. R: A language and environment for statistical computing. R Foundation for Statistical Computing, Vienna, Austria.

Religa, P., Cao, R., Religa, D., Xue, Y., Bogdanovic, N., Westaway, D., Marti, H.H., Winblad, B., Cao, Y., 2013. VEGF significantly restores impaired memory behavior in Alzheimer's mice by improvement of vascular survival. Sci Rep 3, 2053.

Risacher, S.L., Anderson, W.H., Charil, A., Castelluccio, P.F., Shcherbinin, S., Saykin, A.J., Schwarz, A.J., Initiative, A.s.D.N., 2017. Alzheimer disease brain atrophy subtypes are associated with cognition and rate of decline. Neurology 89 (21), 2176–2186.

Saykin, A.J., Shen, L., Foroud, T.M., Potkin, S.G., Swaminathan, S., Kim, S., Risacher, S.L., Nho, K., Huentelman, M.J., Craig, D.W., Thompson, P.M., Stein, J.L., Moore, J.H., Farrer, L.A., Green, R.C., Bertram, L., Jack, C.R., Weiner, M.W., 2010. Alzheimer's Disease Neuroimaging Initiative biomarkers as quantitative phenotypes: Genetics core aims, progress, and plans. Alzheimers Dement 6 (3), 265–273.

Wyman, BT, Harvey, DJ, Crawford, K, Bernstein, MA, Carmichael, O, Cole, PE, Crane, PK, DeCarli, C, Fox, NC, Gunter, JL, Hill, D, Killiany, RJ, Pachai, C, Schwarz, AJ, Schuff, N, Senjem, ML, Suhy, J, Thompson, PM, Weiner, M, Jack Jr, CR, 2013. Alzheimer's Disease Neuroimaging Initiative. Standardization of analysis sets for reporting results from ADNI MRI data. Alzheimers Dement 9 (3), 332–337. doi:10.1016/j.jalz.2012.06.004, MayEpub 2012 Oct 27. PMID: 23110865; PMCID: PMC3891834.

Shaw, L.M., Vanderstichele, H., Knapik-Czajka, M., Clark, C.M., Aisen, P.S., Petersen, R.C., Blennow, K., Soares, H., Simon, A., Lewczuk, P., Dean, R., Siemers, E., Potter, W., Lee, V.M., Trojanowski, J.Q.Alzheimer's Disease Neuroimaging, I., 2009. Cerebrospinal fluid biomarker signature in Alzheimer's disease neuroimaging initiative subjects. Ann Neurol 65 (4), 403–413.

Shaw, L.M., Vanderstichele, H., Knapik-Czajka, M., Figurski, M., Coart, E., Blennow, K., Soares, H., Simon, A.J., Lewczuk, P., Dean, R.A., Siemers, E., Potter, W., Lee, V.M., Trojanowski, J.Q.Alzheimer's Disease Neuroimaging, I., 2011. Qualification of the analytical and clinical performance of CSF biomarker analyses in ADNI. Acta Neuropathol 121 (5), 597–609.

Spellman, D.S., Wildsmith, K.R., Honigberg, L.A., Tuefferd, M., Baker, D., Raghavan, N., Nairn, A.C., Croteau, P., Schirm, M., Allard, R., Lamontagne, J., Chelsky, D., Hoffmann, S., Potter, W.Z.Alzheimer's Disease Neuroimaging, I., Foundation for, N.I.H.B.C.C.S.F.P.P.T., 2015. Development and evaluation of a multiplexed mass spectrometry based assay for measuring candidate peptide biomarkers in Alzheimer's Disease Neuroimaging Initiative (ADNI) CSF. Proteomics Clin Appl 9 (7-8), 715–731.

Spuch, C., Antequera, D., Portero, A., Orive, G., Hernandez, R.M., Molina, J.A., Bermejo-Pareja, F., Pedraz, J.L., Carro, E., 2010. The effect of encapsulated VEGF-secreting cells on brain amyloid load and behavioral impairment in a mouse model of Alzheimer's disease. Biomaterials 31 (21), 5608–5618.

Sweeney, M.D., Montagne, A., Sagare, A.P., Nation, D.A., Schneider, L.S., Chui, H.C., Harrington, M.G., Pa, J., Law, M., Wang, D.J.J., Jacobs, R.E., Doubal, F.N., Ramirez, J., Black, S.E., Nedergaard, M., Benveniste, H., Dichgans, M., Iadecola, C., Love, S., Bath, P.M., Markus, H.S., Salman, R.A., Allan, S.M., Quinn, T.J., Kalaria, R.N., Werring, D.J., Carare, R.O., Touyz, R.M., Williams, S.C.R., Moskowitz, M.A., Katusic, Z.S., Lutz, S.E., Lazarov, O., Minshall, R.D., Rehman, J., Davis, T.P., Wellington, C.L., Gonzalez, H.M., Yuan, C., Lockhart, S.N., Hughes, T.M., Chen, C.L.H., Sachdev, P., O'Brien, J.T., Skoog, I., Pantoni, L., Gustafson, D.R., Biessels, G.J., Wallin, A., Smith, E.E., Mok, V., Wong, A., Passmore, P., Barkof, F., Muller, M., Breteler, M.M.B., Roman, G.C., Hamel, E., Seshadri, S., Gottesman, R.F., van Buchem, M.A., Arvanitakis, Z., Schneider, J.A., Drewes, L.R., Hachinski, V., Finch, C.E., Toga, A.W., Wardlaw, J.M., Zlokovic, B.V., 2019. Vascular dysfunction-The disregarded partner of Alzheimer's disease. Alzheimers Dement 15 (1), 158–167.

Tarkowski, E., Issa, R., Sjogren, M., Wallin, A., Blennow, K., Tarkowski, A., Kumar, P., 2002. Increased intrathecal levels of the angiogenic factors VEGF and TGF-beta in Alzheimer's disease and vascular dementia. Neurobiol Aging 23 (2), 237–243.

Van Dyken, P., Lacoste, B., 2018. Impact of Metabolic Syndrome on Neuroinflammation and the Blood-Brain Barrier. Front Neurosci 12, 930.

Viboolvorakul, S., Patumraj, S., 2014. Exercise training could improve age-related changes in cerebral blood flow and capillary vascularity through the upregulation of VEGF and eNOS. Biomed Res Int 2014, 230791.

Wang, L., Benzinger, T.L., Hassenstab, J., Blazey, T., Owen, C., Liu, J., Fagan, A.M., Morris, J.C., Ances, B.M., 2015. Spatially distinct atrophy is linked to beta-amyloid and tau in preclinical Alzheimer disease. Neurology 84 (12), 1254–1260.

Wang, P., Xie, Z.H., Guo, Y.J., Zhao, C.P., Jiang, H., Song, Y., Zhu, Z.Y., Lai, C., Xu, S.L., Bi, J.Z., 2011. VEGF-induced angiogenesis ameliorates the memory impairment in APP transgenic mouse model of Alzheimer's disease. Biochem Biophys Res Commun 411 (3), 620–626.

Wang, Z., Zhou, W., Zhou, B., Zhang, J., 2018. Association of vascular endothelial growth factor levels in CSF and cerebral glucose metabolism across the Alzheimer's disease spectrum. Neurosci Lett 687, 276–279.

Wiseman, S.J., Doubal, F.N., Chappell, F.M., Valdes-Hernandez, M.C., Wang, X., Rumley, A., Lowe, G.D., Dennis, M.S., Wardlaw, J.M., 2015. Plasma Biomarkers of Inflammation, Endothelial Function and Hemostasis in Cerebral Small Vessel Disease. Cerebrovasc Dis 40 (3-4), 157–164.

Yang, S.-P., Bae, D.-G., Kang, H.J., Gwag, B.J., Gho, Y.S., Chae, C.-B., 2004. Co-accumulation of vascular endothelial growth factor with β-amyloid in the brain of patients with Alzheimer's disease. Neurobiology of Aging 25 (3), 283–290.

Yanovsky, I., Leow, A.D., Lee, S., Osher, S.J., Thompson, P.M., 2009. Comparing registration methods for mapping brain change using tensor-based morphometry. Medical image analysis 13 (5), 679–700.

Yanovsky, I., Thompson, P., Osher, S., Leow, A.D., 2008. Asymmetric and symmetric unbiased image registration: statistical assessment of performance. IEEE Computer Society Workshop on Mathematical Methods in Biomedical Image Analysis 1–8.

Zacchigna, S., Lambrechts, D., Carmeliet, P., 2008. Neurovascular signalling defects in neurodegeneration. Nat Rev Neurosci 9 (3), 169–181.